LIMNOLOGY
and
OCEANOGRAPHY

ASLO

Limnol. Oceanogr. 63, 2018, 741–757

doi: 10.1002/lno.10665

Relative impacts of light, temperature, and reactive oxygen on thaumarchaeal ammonia oxidation in the North Pacific Ocean

Rachel E. A. Horak [1]* Wei Qin,[2] Anthony D. Bertagnolli,[2,a] Alexa Nelson,[1] Katherine R. Heal,[1] Hantten Han,[3] Maija Heller,[3,b] Andrew J. Schauer,[4] Wade H. Jeffrey,[5] E. Virginia Armbrust,[1] James W. Moffett,[3] Anitra E. Ingalls,[1] David A. Stahl,[2] Allan H. Devol[1]

[1]School of Oceanography, University of Washington, Seattle, Washington
[2]Department of Civil and Environmental Engineering, University of Washington, Seattle, Washington
[3]Department of Biological Sciences, University of Southern California, Los Angeles, California
[4]Department of Earth and Space Sciences, University of Washington, Seattle, Washington
[5]Center for Environmental Diagnostics and Bioremediation, University of West Florida, Pensacola, Florida

Abstract

Thaumarchaeota are implicated as the major ammonia oxidizers in the ocean. However, the influence of various abiotic factors in determining their distribution and activity in the upper ocean remain largely unclear. Here, we examined the influence of light, hydrogen peroxide (H_2O_2), and temperature on ammonia oxidation rates for communities dominated by *Thaumarchaeota* at the nitrite maximum across two North Pacific transects. In situ ammonia oxidation was almost exclusively driven by *Thaumarchaeota*, as inferred from ammonia monooxygenase subunit A (*amoA*) genes, *amoA* transcripts, and inhibitor studies. A major shift in population structure near the eastern North Pacific Subtropical Front was revealed by sequence variation of *amoA* genes, showing different *Thaumarchaeota* community structure in oligotrophic gyre and temperate regions. While the most dominant OTUs were closely related, we found significant differences in physiological responses to light and temperature of incubation. At four stations in different biogeochemical regimes, the impact of sunlight intensity and temperature on activity was evaluated using $^{15}NH_4^+$-spiked whole seawater collected from the nitrite maximum and incubated at different depths on a free floating in situ array. Ammonia oxidation was usually completely inhibited by PAR at the surface and 21–45% inhibited at 1% surface PAR, whereas a temperature effect on ammonia oxidation was observed at only two of four stations. While inhibition due to H_2O_2 cannot be ruled out in surface waters, our findings show that below the mixed layer, photoinhibition, and not H_2O_2 toxicity, had a greater influence on ammonia oxidation.

In the ocean, nitrate originating from below the photic zone, or new nitrogen (N_{new}), is an important fuel for new production (Dugdale and Goering 1967). Conversely, nitrate originating from nitrification due to ammonia oxidation within the photic zone fuels regenerated production (Yool et al. 2007). New production relates directly to the export of biological carbon to the deep ocean (the "biological pump"). Because nitrate assimilation is a commonly used measure of new production, it is essential to resolve the relative contributions of N_{new} and regenerated nitrate to surface production (Yool et al. 2007). In order for nitrification to make a significant contribution to regenerated nitrate in surface waters, ammonia oxidizers would need to compete with phytoplankton for ammonia in the photic zone (Martens-Habbena et al. 2009). Measurements of ammonia oxidation activity have routinely demonstrated that nitrification is restricted to the low light levels present at the base of the euphotic zone and deeper (Ward 1985; Santoro et al. 2010; Beman et al. 2012; Horak et al. 2013; Newell et al. 2013; Peng et al. 2015, 2016). However, the assumption that light, and not other limiting factors, exerts primary control over nitrification in the euphotic zone remains largely untested (Smith et al. 2014). In addition, possible ecotypic variability in light sensitivity of different ammonia oxidizing populations has not been explicitly considered, since most measurements

*Correspondence: rahorak@gmail.com

[a]Present address: School of Biology, Georgia Institute of Technology, Atlanta, Georgia

[b]Ifremer, Laboratoire des Cycles Géochimiques, Plouzané, France

Additional Supporting Information may be found in the online version of this article.

of ammonia oxidation are conducted in the dark and without complementary phylogenetic analysis among the contributing populations.

Another possible confounding factor in assessing the contribution of natural variability among nitrifier populations to activity in the photic zone is the recent recognition that some organisms can catalyze both ammonia oxidation to nitrite and nitrite oxidation to nitrate (Daims et al. 2015; van Kessel et al. 2015). Nitrification from NH_4^+ to NO_3^- has historically thought to be dependent upon the concerted activities of both ammonia and nitrite oxidizers. As yet, complete nitrification (comammox) has been documented only in *Nitrospira* species from an aquaculture treatment system and a deep oil well, and no comammox marker gene sequences have been identified in marine waters (Daims et al. 2015). Aerobic ammonia oxidation, therefore, likely remains the rate-limiting step of nitrification in marine systems.

Consistent with earlier predictions from molecular and kinetic studies, direct measurements of the relative contribution of marine ammonia-oxidizing Archaea (AOA) and ammonia oxidizing bacteria (AOB) to in situ ammonia oxidation indicated that AOA are almost exclusively responsible for ammonia oxidation in ammonium-limited oceanic waters (Martens-Habbena et al. 2015; Peng et al. 2015). In addition, members of marine AOA, affiliated with the order *Nitrosopumilales* within the phylum *Thaumarchaeota* (Qin et al. 2015*b*,*c*), greatly outnumber ammonia-oxidizing bacteria (AOB) in ammonia-limited marine waters (Santoro et al. 2010; Beman et al. 2012; Horak et al. 2013; Newell et al. 2013; Martens-Habbena et al. 2015; Peng et al. 2016), and AOA populations can comprise up to 40% of microbiota in the meso- and bathypelagic zones (Karner et al. 2001; Sintes et al. 2013). Although AOA are now recognized to have a central role in marine nitrification, relatively little is known about the environmental variables influencing their distribution and activities in the open ocean.

The influence of abiotic variables on environmental distributions and activity of AOA have mostly been drawn from ecophysiological characterization of the few available pure and enrichment cultures (Martens-Habbena et al. 2009; Amin et al. 2013; Qin et al. 2014; Bayer et al. 2016), but culture studies do not always agree with similar studies of natural populations of marine AOA. For instance, the effect of temperature on ammonia oxidation rates in pure cultures of marine AOA differ from that observed in natural marine populations. Culture-based analyses by Qin et al. (2014) showed Q_{10} values of 2.89, 2.62, and 2.49 for marine AOA isolates SCM1, HCA1, and PS0 (provisionally assigned to the new species *Nitrosopumilus cobalaminigenes* and *Nitrosopumilus ureiphilus*, respectively; Wei Qin et al. unpubl.), respectively, whereas both Horak et al. (2013) and Baer et al. (2014) reported no effect of temperature on ammonia oxidation rates in natural populations. The disagreement could derive from an aggregated response of multiple thaumarchaeotal genotypes present in a sampled water volume, masking possible physiological variability among individual environmental populations. The disagreement could also reflect the physiological status of AOA in natural environments, where AOA likely grow slowly and multiple factors could limit growth.

Previous laboratory and environmental studies indicate that low ammonia availability and competition with phytoplankton and heterotrophs for regenerated ammonia in the upper water column should not be primary limiting factors for AOA in the open North Pacific Ocean (Martens-Habbena et al. 2009; Peng et al. 2016). Notably, high affinities for ammonia and oxygen revealed in culture (Martens-Habbena et al. 2009; Qin et al. 2015*a*, 2017) are generally consistent with direct kinetics measurements of marine environments in which AOA dominate, where ammonia oxidation has been associated with exceptionally low K_m values for ammonia (as low as 22.8 nmol L^{-1}, lower limit of error, total ammonia plus ammonium) and oxygen (as low as 203 nmol L^{-1}) (Bristow et al. 2016; Peng et al. 2016). The high substrate affinities of marine AOA reflect their remarkable adaptation to growth under conditions of constantly low energy flux. This is thought to provide a competitive advantage relative to AOB, and is consistent with the high activity and abundance of marine AOA observed in subsurface waters of nutrient-limited marine environments, such as the oligotrophic gyre (Mincer et al. 2007; Sintes et al. 2013) and in oxygen deficient zones (Peng et al. 2015, 2016). Thus, photosensitivity is possibly a more relevant controlling variable in the open ocean.

Marine AOA abundance and ammonia oxidation rates show generally consistent negative relationships with ambient light intensity in diverse geographical regions (Mincer et al. 2007; Beman et al. 2012; Horak et al. 2013; Newell et al. 2013). The highest ammonia oxidation rates and AOA *amoA* (ammonia monooxygenase subunit A) gene or transcript abundance in depth profiles usually coincides with the depth of the primary nitrite maximum, found at the base of the euphotic zone throughout the world ocean (Beman et al. 2008, 2012; Horak et al. 2013; Santoro et al. 2013). In fact, the photosensitivity of ammonia oxidation in the oceans is a frequently cited model for the formation of the primary nitrite maximum (Lomas and Lipschultz 2006). However, a recent study by Smith et al. (2014) reported that light did not have an inhibitory effect on ammonia oxidation in California coastal waters. The "Water Column A" or Group A *Thaumarchaeota* genotypes of the marine AOA (also known as the shallow AOA ecotype, labeled Group A in Fig. 4) in their study sites appeared to be light-tolerant and were able to maintain similar or even higher ammonia oxidation rates at high irradiance intensities compared to dark controls of the same population (Smith et al. 2014). In addition, recently published studies of light sensitivity of AOA in culture have shown significant variability among phylogenetically closely related marine AOA strains (Qin et al. 2014).

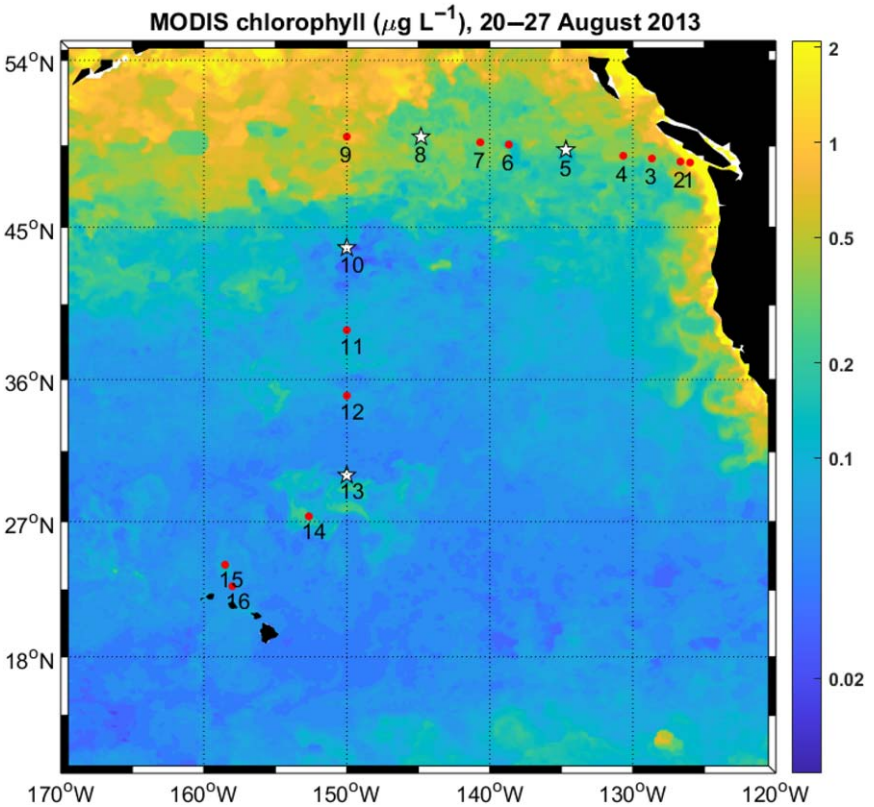

Fig. 1. Map of sampling stations in the North Pacific Ocean. Color indicates MODIS chlorophyll (μg L^{-1}) from 20 August 2013 to 27 August 2013 (http://orca.science.oregonstate.edu/1080.by.2160.8day.hdf.chl.modis.php).

Photoinhibition may also arise indirectly if photochemically produced species, such as hydrogen peroxide (H_2O_2), adversely affect the physiology of AOA. Tolar et al. (2016) demonstrated that H_2O_2 negatively affected ammonia oxidation rates in the ocean, and the effect appeared to be region and taxa specific. However, although the genome of *Nitrosopumilis maritimus* reveals no peroxidase or catalase genes (Walker et al. 2010), it is not inhibited by relatively high concentrations of hydrogen peroxide (Qin et al. 2017). Therefore, light remains a poorly constrained variable controlling nitrate regeneration within the photic zone. Here, we use in situ bottle incubations under different temperature and light intensities to examine the relationships between AOA phylotype, temperature, light intensity, and ammonia oxidation rates in the North Pacific, and to directly compare photoinhibition with H_2O_2 distribution and toxicity. Consistent with culture-based analyses, natural communities of closely related AOA phylotypes displayed significant variation in sensitivity to these environmental parameters.

Methods

Sample collection and hydrographic analysis

We conducted photosensitivity, temperature, and H_2O_2 amendment experiments aboard the R/V *Kilo Moana* on cruise KM1314 (06 August 2013–05 September 2013) at four stations (5, 8, 10, and 13) across the North Pacific Ocean (Fig. 1; Table 1). Surface MODIS chlorophyll during the sampling period is shown in Fig. 1. Water was collected using a conductivity–temperature–depth (CTD) rosette fitted with 10-L Niskin bottles and equipped with a Seabird SBE CTD sensor package and WETLabs ECO FLNTU fluorometer. Oxygen concentrations were measured with the CTD sensor package (SBE-43) and calibrated against Winkler dissolved oxygen determinations ($n = 65$; $R^2 = 0.98$).

Within an hour of sample collection, NH_4^+ concentrations were measured using the o-phthaldialdehyde fluorescence method (standard concentration range: 0–1000 nmol L^{-1}, $n = 6$ standards) (Holmes et al. 1999) and NO_2^- was measured using spectrophotometry (standard concentration range: 0–800 nmol L^{-1}, $n = 6$ standards) (Grasshoff et al. 1999). The detection limit for both was 10 nmol L^{-1}. Samples for NO_3^- were filtered (0.22 μm) and frozen at −20°C until shore-based analysis (UNESCO 1994), and the detection limit was 50 nmol L^{-1}.

Light measurements

Incident solar irradiance was monitored using a Biospherical Instruments (San Diego, California) GUV-511. Underwater profiles were measured using a Biospherical Instruments

Table 1. Hydrographic data for the photoinhibition, temperature, and hydrogen peroxide experiments. Water depth indicates the location at which water was taken for the experiments.

Station	Longitude (°W)	Latitude (°N)	Sample depth (m)	% surface PAR	Temperature (°C)	Fluorescence (mg m^{-3})	$[O_2]$ (μmol L^{-1})	$[NH_4^+]$ (μmol L^{-1})	$[NO_2^-]$ (μmol L^{-1})	$[NO_3^-]$ (μmol L^{-1})
5	134.70	49.30	85	0.12	6.8	0.24	277.2	0.06	0.35	2.7
8	144.80	50.00	65	0.24	5.4	1.52	283.9	<0.01	0.36	15.6
10	150.00	43.83	100	0.19	9.1	0.67	264.2	0.02	0.02	6.7
13	150.00	30.00	170	0.07	17.4	0.15	197.9	0.01	0.03	1.6

PUV-500 paired with the GUV-511 radiometer. In addition, there was a CTD-mounted PAR sensor (QSP-2100; Biospherical Instruments). While both a PUV and QSP were used to measure underwater irradiance, the two instruments are not easily comparable (Kirk 1994), because the PUV uses a cosine collector and is limited to downwelling irradiance while the QSP-2100 uses a 4π collector.

We used measurements from the PUV/GUV pair to determine % PAR at depth. Multiple PUV profiles were conducted near solar noon. Attenuation coefficients (K_d) were calculated using the Beer-Lambert law (Kirk 1994). Percent irradiance at depth was determined by direct comparison between simultaneous measurements from the PUV and GUV instruments. Percent irradiances below the profiles' maximum depth ($\sim$ 70 m) were calculated from the exponential equation determined directly from the measured data.

We also estimated maximum quantum flux (μE m^{-2} s^{-1}) for both the PUV/GUV pair and QSP sensor. For the PUV/GUV pair, we calculated maximum quantum flux by first assuming that 1/3 of incident light from GUV measurements was attenuated at the air–water interface, and then calculating quantum flux at depth using the Beer-Lambert law. We used the 1-m depth binned PAR data from the CTD-mounted 4π QSP PAR sensor as the maximum quanta flux for quantum scalar irradiance.

H_2O_2 measurements

Samples for in situ H_2O_2 profiles were analyzed at sea within 1–2 h of collection using a flow injection chemiluminescence (FIA-CL) reagent injection method (Yuan and Shiller 1999) as described previously (Croot et al. 2004). Samples were analyzed using five replicates: typical precision was 2–3% from 0.5 nmol L^{-1} to 150 nmol L^{-1}, the detection limit (3 σ) was typically 0.2 nmol L^{-1}.

Quantitative PCR analysis and cell counts

Quantitative-PCR (q-PCR) and reverse transcription q-PCR (RT-q-PCR) were used to estimate the abundance of archaeal and bacterial *amoA* genes and transcripts, respectively. The procedure exactly followed Heal et al. (2017). Briefly, water samples for q-PCR (1 L) and RT-q-PCR (4 L) were retrieved from the NO_2^- maximum of each station and filtered through 0.22 μm Sterivex filter (GP-type, Millipore). In the laboratory, environmental DNA and RNA were extracted as described previously (Urakawa et al. 2010; Horak et al. 2013; Martens-Habbena et al. 2015). The primer sets used for targeting AOA *amoA* genes and transcripts were CrenAmoAQ-F and CrenAmoAModR (Mincer et al. 2007). AOB *amoA* genes and transcripts were amplified using the primer sets amoA1F and amoA2R (Rotthauwe et al. 1997). The copy numbers of AOA and AOB *amoA* genes and transcripts were quantified in triplicate in a capillary system (LightCycler, Roche) using the cycling conditions described previously (Horak et al. 2013). Water samples for cell counts were collected from the same depth on the same cast as samples for q-PCR analyses and fixed with glutaraldehyde (final concentration 2% (vol/vol)). After filtration of 1 mL of sample onto a 0.02-μm-pore-size Anodisc 25 filter (Whatman), cells were stained with Moviol-SybrGreen mix (Lunau et al. 2005), and total prokaryotic cell numbers were counted with an Olympus BHS/BHT system microscope. At least 20 random fields of view with 10–100 SybrGreen stained cells per field were counted.

AOA community diversity

We determined archaeal community diversity in water samples collected from the NO_2^- maximum samples at Sta. 1, 3, 5, 8, 10, 11, 13, 14, 15, 16. Thaumarchaeal *amoA* genes were amplified from template DNA ($\sim$ 20 ng μL^{-1}) using a two-step enrichment procedure for target amplication and sample barcoding on a Fluidigm Access Array (Fluidigm, San Francisco, California). Gene targets were amplified using primer pairs ArchAmoA_1F and ArchAmoA_1R and sample specific GoLay primers (Francis et al. 2005). Amplified products were analyzed by gel electrophoresis to ensure the correct amplicon size, quantified using pico-green, pooled to a equal molar concenctration and sequenced in pair-end 300 bp mode using the Illumina HiSeq Platform. Resulting sequences were assessed for quality using fastq_eestats and trimmed at the 5′ (5 bp) and 3′ (225 bp) ends (Edgar 2010). Trimmed reads were then quality filtered in QIIME using the recommendations described by Bokulich et al. (2013). The resulting reads were then analyzed using the UPARSE pipeline with an OTU clustering identity of 95% (Edgar 2013). Represenative OTU sequences were analyzed against a reference database of Thaumarchaeal amoA sequences in the ARB software using the parsimony tool for insertion (Ludwig et al. 2004; Pester et al. 2012). Sample-OTU matrices from

UPARSE were converted to biom format and rarified to 1000 reads per sample using the single_rarfy.py script in QIIME. The resulting output file was then used for calculation of Bray–Curtis similarity values between samples and hiearchical clustering using the package vegan in R.

Application of selective metabolic inhibitors of ammonia oxidation

At Sta. 5 and 8, we used selective inhibitors, ATU (allylthiourea) and PTIO (2-phenyl-4,4,5,5,-tetramethylimidazoline-1-oxyl-3-oxide), to assess the relative contribution of AOB and AOA to ammonia oxidation at the NO_2^- maximum (Martens-Habbena et al. 2015). AOB are more sensitive to ATU, while AOA are more sensitive to PTIO (Martens-Habbena et al. 2015; Sauder et al. 2016). Water for the inhibitor experiments was collected on the same day (within 12 h) and at the same depth as the photoinhibition experiments. We combined ^{15}N-ammonia oxidation rate measurements with inhibitor treatments as previously described (Martens-Habbena et al. 2015), incubated samples in 125 mL Nalgene bottles, and compared results of inhibitor treatments to three negative control (no inhibitors) samples. Concentrations of ATU ranged from 10 μmol L^{-1} to 500 μmol L^{-1} (six treatments) and concentrations of PTIO ranged from 2 μmol L^{-1} to 250 μmol L^{-1} (eight treatments). All treatments were conducted in triplicate. Two positive control treatments contained both PTIO and ATU at different concentrations: (1) 250 μmol L^{-1} PTIO + 500 μmol L^{-1} ATU, and (2) 100 μmol L^{-1} PTIO + 100 μmol L^{-1} ATU. None of the positive controls had measurable ammonia oxidation rates. Samples were incubated for 24–25 h in the dark at in situ temperatures. At the end of the incubation, a 20 mL subsample was flash frozen at −80°C for δ^{15}N-$NO_2^- + NO_3^-$ analysis.

The cadmium azide method was used to reduce NO_3^- and NO_2^- to N_2O, and the ^{15}N label in recovered N_2O was determined by isotope ratiomass spectrometry (IRMS; McIlvin and Altabet 2005). Sample preparation for IRMS, analysis, and rate calculations exactly followed Horak et al. (2013).

Photoinhibition and temperature experiment

A light bottle/dark bottle comparison study design was used for the photoinhibition experiment. At four stations (5, 8, 10, 13), water was collected from the CTD rosette several hours prior to dawn from a single depth, the NO_2^- maximum, or 15 m below if fluorescence was substantial (> 1.0 mg m^{-3}) at the NO_2^- maximum (Table 1). Acid-washed, Milli-Q water rinsed, clear 1 L polycarbonate Nalgene bottles (total volume = 1.234 L) were filled by overflowing 2–3 volumes and capping the bottle with as little headspace as possible. We then added 50 nmol L^{-1} $^{15}NH_4^+$ to all samples as close to deployment of the array as possible, and gently inverted to evenly distribute $^{15}NH_4^+$. Dark treatment bottles were assembled by covering the bottles with two heavy-duty black trash bags. All samples were kept in the dark until deployment on a free floating array. Three clear bottles and three dark bottles were attached within 1 m of each other to a free floating in situ array, which was deployed at sunrise. Triplicate samples were incubated at five different depths, ranging from the surface to 190 m, and subjected to in situ light and temperature during incubation. The free floating array was recovered at sunset (incubation time varying from 13.4 to 15.2 h), and a 20 mL subsample from each bottle was flash frozen at −80°C immediately for δ^{15}N-$NO_2^- + NO_3^-$ analysis (see above for cadmium azide method).

The photoinhibitory effect is generally expressed as % inhibited at a particular depth, where % inhibited = ((average dark rate at depth z – average light rate at depth z)/average dark rate at depth z) × 100. For consistency with prior studies (Horak et al. 2013), rates are calculated for a 24 h period and assume that daylight rates are representative of rates over a 24 h period. Rates calculated for bottles incubated in the light (clear bottles) are likely to be underestimates of the daily ammonia oxidation rate because of expected recovery of ammonia oxidation at night. Calculated % inhibition is equivalent to the inhibition expressed during the light period.

H_2O_2 amendment experiments

The effect of H_2O_2 on nitrification was studied using samples collected with a trace metal clean rosette and teflon coated "Niskin-type" bottles with external springs (Ocean Test Equipment). These precautions were important to avoid secondary effects arising from peroxide – metal interactions. Clear 1 L polycarbonate bottles (Nalgene) were covered with duct tape to avoid light. Niskins were sampled in a positive pressure clean van using teflon tubing. In order to maintain the ambient oxygen, 2–3 L were overflowed and bottles capped with as minimal headspace as possible. For each analysis, we added 50 nmol L^{-1} $^{15}NH_4^+$ and 50 nmol L^{-1} H_2O_2 for the peroxide treatment ($n = 3$) and only $^{15}NH_4^+$ to the control group ($n = 3$). This concentration was selected as representative of H_2O_2 at the base of the mixed layer throughout much of the cruise, so it represented a realistic intermediate value, and is comparable to the range of 10–300 nmol L^{-1} used by Tolar et al. (2016). Following addition, the bottles were gently inverted to ensure that the hydrogen peroxide solution and $^{15}NH_4^+$ were evenly distributed and incubated for 24–25 h in the dark at in situ temperatures in a temperature-controlled room. At the end of the incubation, 20 mL subsamples were flash frozen at −80°C for δ^{15}N-$NO_2^- + NO_3^-$ analysis (see above for cadmium azide method).

N uptake experiments

Ammonia oxidation rate measurements can be sensitive to N uptake rates if a significant amount of ammonia, or the $^{15}NO_2^-$ or $^{15}NO_3^-$ produced by nitrification, is taken up into the particulate fraction (Ward 2011). We conducted two types of N uptake experiments to evaluate the possible influence of assimilation on measured ammonia oxidation rates. At Sta. 13, we determined NH_4^+ uptake in samples taken

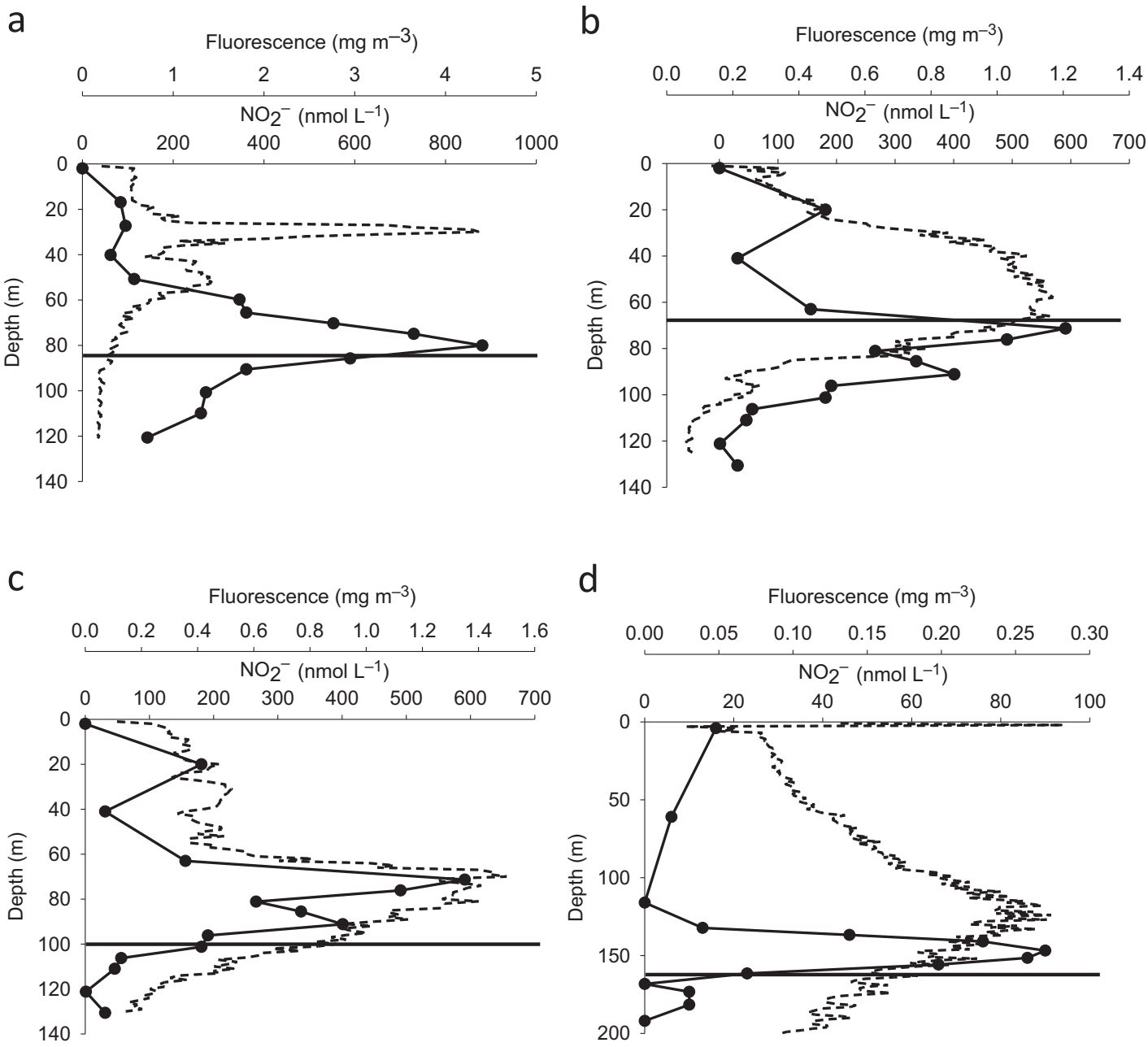

Fig. 2. NO_2^- and fluorescence measurements at stations examined in the photoinhibition experiments: (**a**) Sta. 5, (**b**) Sta. 8, (**c**) Sta. 10, (**d**) Sta. 13. NO_2^- is indicated by the solid line, and fluorescence is indicated by the dashed line. The horizontal line is the depth from which water was taken for the ammonia oxidation rates experiments.

from bottles at the termination of the photoinhibition experiment (called "post-photoinhibition N uptake experiment"). Water from the three replicates of each treatment (depth and light/dark) was pooled and filtered onto a single 0.3 μm GF75 filter. This resulted in a single N uptake replicate for each treatment.

At Sta. 5, 8, 10, and 13, we measured both NH_4^+ and NO_2^- uptake into particulate matter with water collected independently of the photoinhibition experiments, but conducted on the same day. Whole seawater was collected into clear 2-L Nalgene bottles and capped with as little headspace as possible. Separate bottles were used to measure uptake of NH_4^+ (addition of 50 nmol L^{-1} $^{15}NH_4^+$) and NO_2^- (addition of 50 nmol L^{-1} $^{15}NO_2^-$). Following addition, the bottles were covered with three layers of neutral density screening to simulate the light intensity of the NO_2^- maximum and incubated for 6–8 h in surface seawater deck incubators. Aliquots were filtered onto 1.6 μm GF/A and 0.3 μm GF75 in series (to

Table 2. Cell, genes, and transcript abundance of AOA and *β*-AOB *amoA*. The cell number, gene abundances, total and per-cell AOA *amoA* transcript abundances and total prokaryotes numbers are for the primary NO_2^- maxima of each station (the depth at which water was taken for the photoinhibition and temperature experiments). Note: AOB *amoA* transcript copy number was below the limit of detection.

Stations	AOA *amoA* gene abundance (copies mL^{-1})	*β*-AOB *amoA* gene abundance (copies mL^{-1})	AOA *amoA* transcript abundance (copies mL^{-1})	Total prokaryotes number (mL^{-1})	Cell abundance ratio AOA/AOB*	AOA (% of total prokaryotes)†	AOB (% of total prokaryotes)‡	AOA *amoA* transcript per gene copy
5	1.48×10^5	7.59×10^3	5.59×10^4	2.26×10^5	48.71	65.42	0.060	0.38
8	3.45×10^4	1.52×10^3	1.64×10^4	2.99×10^5	56.84	11.56	0.063	0.47
10	4.41×10^4	2.15×10^3	4.69×10^4	4.01×10^5	51.25	11.01	0.015	1.06
11	1.32×10^5	3.68×10^3	4.30×10^4	3.25×10^5	89.82	40.66	0.011	0.32
13	3.03×10^4	9.92×10^2	9.30×10^3	1.14×10^5	76.50	26.74	0.031	0.31
16	3.93×10^4	1.39×10^3	6.46×10^3	ND	70.73	ND	ND	0.16

ND, not determined.
*,†,‡ Ammonia oxidizer cell numbers were derived from *amoA* gene abundances, assuming an average of 1 *amoA* gene copy per AOA genome and 2.5 *amoA* gene copies per *β*-AOB genome.

separate large phytoplankton, diatoms, from small plankton) before being flash frozen at −80°C and stored at −20°C. For both experiments, we subsampled T_0 samples just after the addition of labelled N to account for sorption onto the filters.

Filters from both experiments were dried and packed into tin capsules ashore. Samples were analyzed by Elemental Analysis – Isotope Ratio Mass Spectrometry (EA-IRMS; Finnigan MAT251 Isotope Ratio Mass Spectrometer), which yielded both the amount of particulate N and the isotope ratio of the particulate N in each sample. Nitrogen uptake rates were calculated according to Bronk et al. (1994).

Results

Hydrographic data

All samples were taken from the NO_2^- maximum, which was below the chlorophyll maximum (Fig. 2). Concentrations of NH_4^+ and NO_2^- were low at all locations. NH_4^+ ranged from undetectable (less than 10 nmol L^{-1}) to 60 nmol L^{-1}, NO_2^- ranged from 20 nmol L^{-1} to 360 nmol L^{-1} (Fig. 2), and NO_3^- ranged from 1.6 μmol L^{-1} to 15.6 μmol L^{-1} (Table 1). Chlorophyll fluorescence was low for all samples, ranging from 0.15 mg m^{-3} to 1.3 mg m^{-3} (Figs. 1, 2).

Abundance and expression of archaeal and betaproteobacterial *amoA* genes

AOA and *β*–AOB were quantified around the primary NO_2^- maximum of each station based on *amoA* gene abundance. Thaumarchaeal *amoA* abundances ranged from 3.03×10^4 to 1.48×10^5 copies mL^{-1} (Table 2). Assuming an average of 1 *amoA* gene copy per AOA genome (Stieglmeier et al. 2014), thaumarchaeal abundance in North Pacific waters collected near the NO_2^- maximum (11–65% of all prokaryotes) was 49–90 fold greater than *β*–AOB abundance, assuming that there are 2–3 *amoA* gene copies per *β*–AOB genome (Table 2; Norton et al. 2002). Betaproteobacterial AOB accounted for less than 0.6% of total prokaryotic population. Similarly, thaumarchaeal *amoA* transcript abundances at the NO_2^- maximum greatly exceeded that of *β*–AOB, varying between 6.46×10^3 and 5.59×10^4 copies mL^{-1} (Table 2). Betaproteobacterial *amoA* transcript abundances were below detection limits for all four stations (data not shown). The ratio of AOA *amoA* transcripts per gene copy varied from 0.16 to 1.06.

AOA community diversity

Overall, we recovered 40 unique AOA *amoA* OTUs (95% nucleotide identity cutoff). All AOA *amoA* sequences were affiliated with Group A (Francis et al. 2005; Nunora et al. 2015) but were distributed among different lineages of Group A at each Station (Figs. 3, 4). OTU_1 represented one of the dominant groups of marine AOA at a coastal station (Sta. 1) but was detected in much lower relative abundance in oceanic stations. The dominant *amoA* OTU types

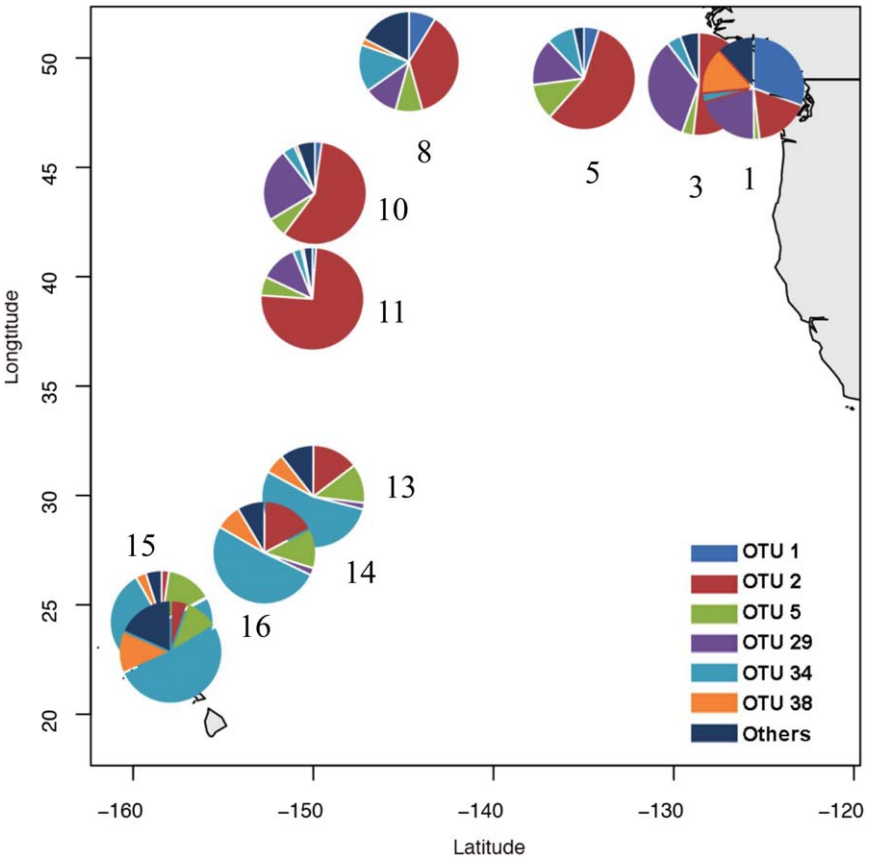

Fig. 3. Proportional representation of Thaumarchaeal *amoA* OTUs (*amoA* gene amplicon) community diversity at the experimental depth, the NO_2^- maximum.

(OTU_2, OTU_5, OTU_29, and OTU_34) at the NO_2^- maximum were affiliated with two lineages within one subclade of Group A (Figs. 3, 4). The greatest divergence in AOA population structure was observed between major ocean biogeochemical regimes separated by the Eastern North Pacific Subtropical Front, marking the transition from the so-called high nitrate-low chlorophyll (HNLC) waters of the north into the oligotrophic gyre (Supporting Information Fig. S1; ANOSIM, $R = 0.81$, $p < 0.05$). The AOA community in the oligotrophic gyre was dominated by OTU_5 and OTU_34, comprising $\sim$ 60–80% of all sequence tags, whereas water samples from temperate regions were mainly composed of OTU_2 and OTU_29 (Figs. 3, 4), comprising 50–80% of all sequence tags.

Metabolic inhibitors experiments

Selective inhibitor studies using ATU and PTIO showed that the ammonia oxidizing community is much more sensitive to PTIO than ATU. The community response at Sta. 5 and 8 to ATU and PTIO was similar to two AOA isolates (*Nitrosopumilus maritimus* strain SCM1 and a recently described AOA isolate strain HCA1, provisionally assigned to the new species *Nitrosopumilus cobalaminigenes*; Wei Qin et al. unpubl.), and distinct from the response of AOB in culture (Supporting Information Fig. S2). This is fully consistent with the molecular data, together attributing almost all of the community ammonia oxidation to marine AOA.

Photoinhibition experiments

Light attenuation was similar among stations (Fig. 5; Supporting Information Table S1). The light attenuation curve accounts for the fact that at least 30% of incident light is lost near the water/air interface (Kirk 1994), therefore, % surface PAR ranged from less than 40–60% at the shallowest depth measured (2 m). Percent surface PAR at the depth of water collected for the photoinhibition experiment (NO_2^- maximum) was always below 1% surface PAR, and ranged from 0.07% (Sta. 13) to 0.24% (Sta. 8; Table 1). The PAR measurements listed in Table 3 are the maximum value for that day, and do not provide information of varying exposure to light during the period of incubation. The calculated maximum photon flux that the incubation experienced in the clear bottle (light treatment) differed for the PUV radiometer and CTD mounted 4π PAR sensor (Supporting Information Table S1). This is to be expected based on the different shapes of the detectors.

AQ10

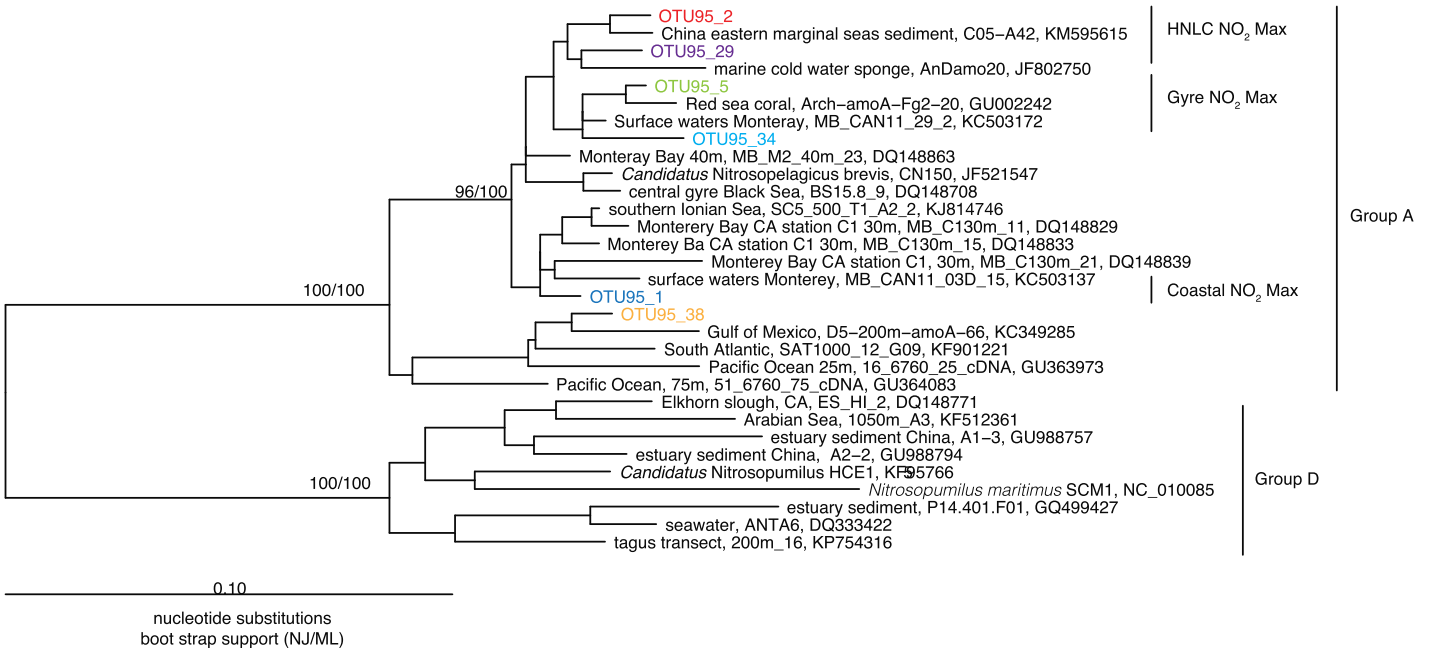

Fig. 4. The phylogenetic approximation of AOA Thaumarchaeal *amoA* OTUs (*amoA* gene amplicon) community diversity at the experimental depth, the NO_2^- maximum. High-scoring pairs (top hits only) to each OTU from the *amoA* ARB-database reported by Pester et al. (2012) are displayed (black). Boot-strap support values of 70% or greater are displayed and based on neighbor-joining analysis with 1000 re-samplings of partial full-length sequences (600 bp or greater) only. OTUs from this survey were placed within the reference tree using parsimonious placement in the ARB software package. Proportional representation of each OTU is based on sample matrices rarified to 1000 sequences per sample. Y-axes represent proportional representation.

Ammonia oxidation at all four stations varied with varying PAR (Fig. 5; Supporting Information Table S1). Ammonia oxidation in clear bottles was undetectable or minimal at the surface (compared to dark bottles). Ammonia oxidation rates at the surface and 12 m for Sta. 8 and 13 were not significantly different from zero. In contrast, ammonia oxidation rates in clear and dark bottles were indistinguishable in water samples collected from the NO_2^- maximum and deeper, indicating little to no photoinhibition at these depths. Mean attenuation of inhibition with depth associated decrease in PAR is described by a strong linear trend (Fig. 6; regression analysis; Sta. 5: $p < 0.001$, $R^2 = 0.990$; Sta. 8: $p < 0.001$, $R^2 = 0.986$; Sta. 10: $p = 0.013$, $R^2 = 0.975$; Sta. 13: $p = 0.003$; $R^2 = 0.966$). Also, regression analysis indicates that at 1% surface PAR (sPAR), ammonia oxidation rates were inhibited 25–41% by sunlight in clear bottles. Notably, the inhibitory response of ammonia oxidation by light varied between stations (ANCOVA; $p < 0.005$; group A: Sta. 5, 10, 13; group B: Sta. 5 and 8), pointing to significant physiological variation in response to PAR among natural populations at four stations spanning coastal zones to the subtropical gyre.

Effect of temperature on ammonia oxidation rates

At each station, a comparison of the dark treatment rates yielded additional data on the effect of temperature on the ammonia oxidation rate, as samples were exposed to a range of in situ temperatures. There was a 9.6–10.8°C difference between the highest and lowest temperature treatments (Fig. 2; Table 3). There was no significant difference in the dark treatment ammonia oxidation rate with samples incubated at five different in situ temperatures at Sta. 5 and 10 (Fig. 5; one-way ANOVA: Sta. 5, $p = 0.447$; Sta. 10, $p = 0.593$). In contrast, the ammonia oxidation rate appeared sensitive to temperature at Sta. 8 and 13, where the rate at the surface was higher than at depth (Fig. 5; one-way ANOVA; Sta. 8, $p = 0.008$; Sta. 13, $p = 0.033$). The observed Q_{10} for ammonia oxidation at Sta. 8 and 13 was 1.7 and 3.4, respectively.

In situ H_2O_2 concentrations and H_2O_2 amendment experiments

Hydrogen peroxide depth profiles were similar to those reported elsewhere in temperate and subtropical gyres (Fig. 7; Heller et al. 2013), detectable throughout the depth range, but it was highest in the mixed layer. Addition of H_2O_2 to a concentration (50 nmol L^{-1}) significantly exceeding ambient concentrations did not inhibit ammonia oxidation in any of the 15 samples examined (Supporting Information Table S2). However, there was an unexpected significant increase in rates in 5 of 15 samples.

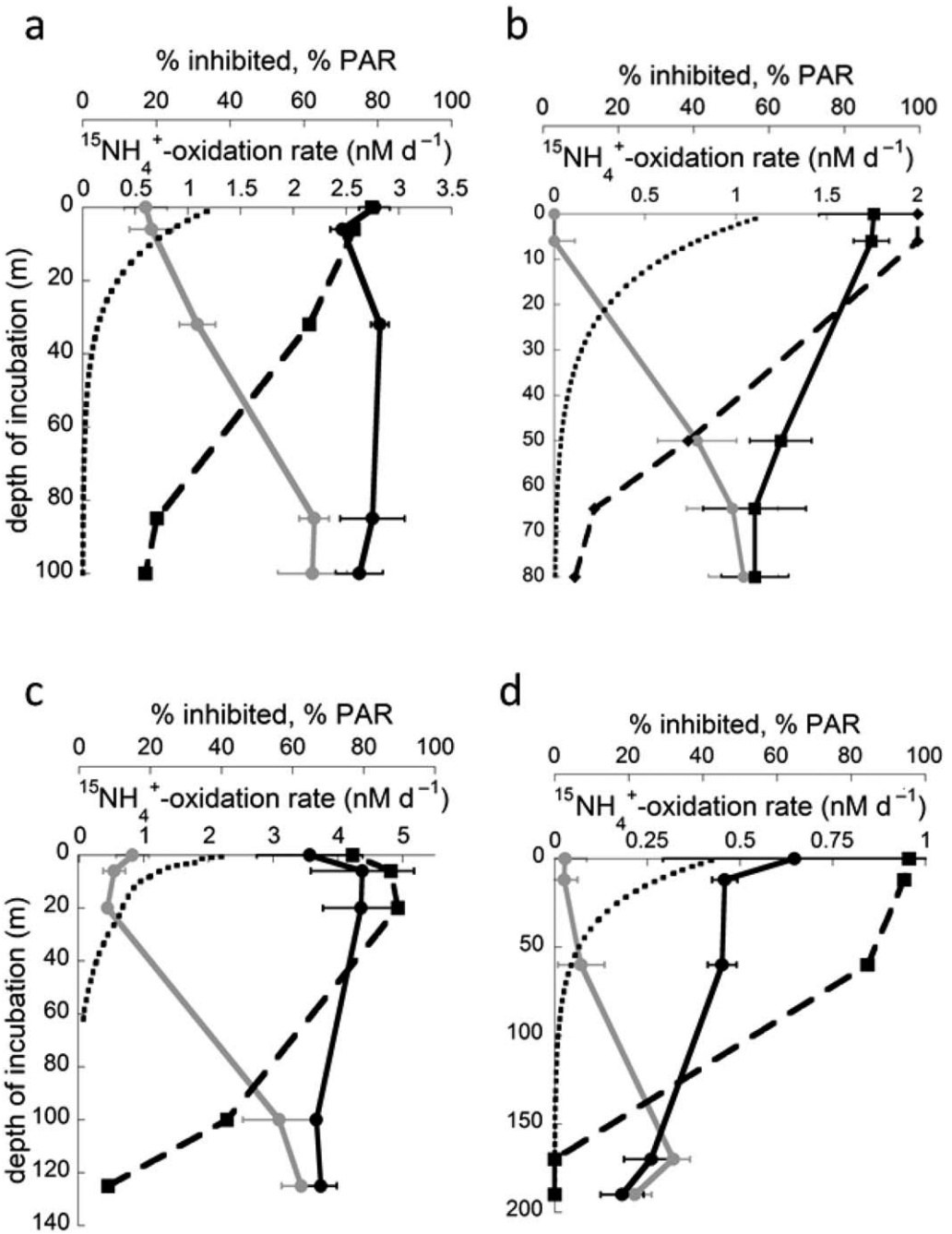

Fig. 5. Results of photoinhibition experiments at (**a**) Sta. 5 (sampling depth: 85 m), (**b**) Sta. 8 (sampling depth: 65 m), (**c**) Sta. 10 (sampling depth: 100 m), (**d**) Sta. 13 (sampling depth: 170 m). For all panels, the dotted line = % surface PAR (measured with PUV radiometer); gray line = ammonia oxidation rate for the light treatment; solid black line = ammonia oxidation rate for the dark treatment; dashed line = % inhibition. Data are mean ± 1 standard deviation, $n = 3$.

N uptake experiments

The post-photoinhibition NH_4^+ uptake experiment at Sta. 13 showed that NH_4^+ uptake was much lower in the light treatment than the dark treatment at the highest light conditions (surface and 12 m; Supporting Information Fig. S3). In the more traditional N uptake experiments, total NO_2^- uptake rates (1.6 μm + 0.3 μm size fraction uptake rates) were generally one to two orders of magnitude lower than ammonia oxidation rates from the same water depth (0.02–0.26 nmol L^{-1} d^{-1}; Supporting Information Table S3). At lower light conditions (60 m, 170 m, and 190 m), NH_4^+ uptake in the light treatment was the same or higher than

Table 3. Station variation in Q_{10} for environmental populations.

Station	Temperature range (°C)	Q_{10}
5	6.5–16.4	1.0
8	5.0–14.6	1.7
10	8.4–18.1	1.0
13	15.5–26.3	3.4

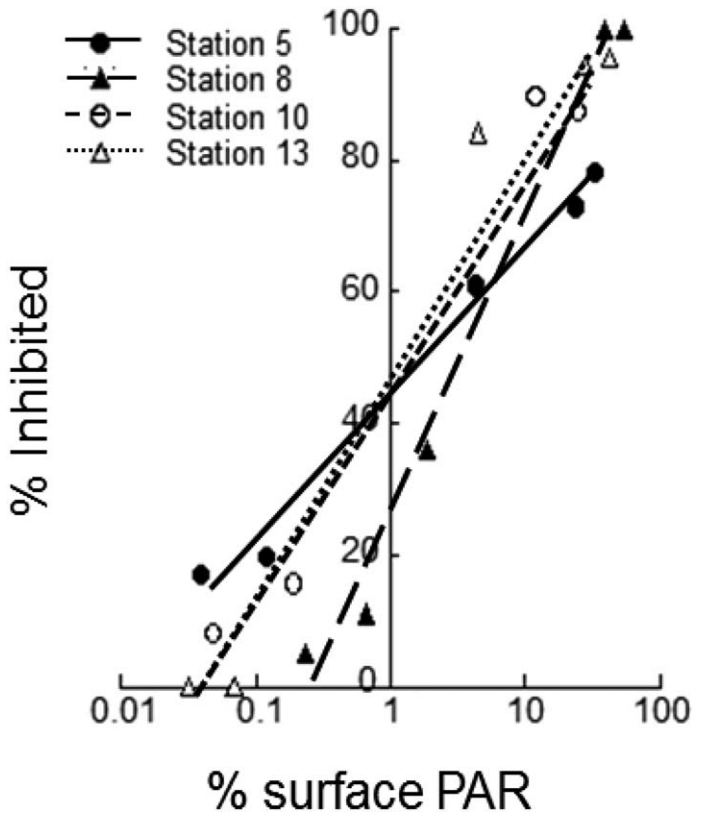

Fig. 6. Comparison of light inhibition for all study stations. Closed circle and solid line = Sta. 5; closed triangle and solid line = Sta. 8; open circle and dashed line = Sta. 10; open triangle and dotted line = Sta. 13. Lines are linear regression analysis. Note: *x*-axis is log scale.

the dark treatment (Supporting Information Fig. S3). Total NH_4^+ uptake rates (1.6 μm + 0.3 μm size fraction uptake rates) at depths near the chlorophyll maximum (Sta. 8) or NO_2^- maximum (Sta. 5, 10, 13) ranged from 3.05 nmol L^{-1} d^{-1} to 95.56 nmol L^{-1} d^{-1} (Supporting Information Table S3).

Discussion

AOA community diversity by station

AOA community diversity was determined at the NO_2^- maximum for all stations, and was approximately 15 m above the depth of the photoinhibition experiments at Sta. 10 and 13. As such, we cannot exclude the possibility that the population structure at the depth of the photoinhibition experiments is slightly different. However, because the dominant *amoA* OTU types were affiliated to two closely related lineages of group A at the NO_2^- maximum of all sampled stations across two transects, it is likely that marine AOA communities were also dominated by those closely related shallow group phylotypes at the photoinhibition experimental depths at Sta. 10 and 13.

With the very clear and fine-scale mapping of phylotypes to presumptive ecotypes evident along the two major cruise transects, we can now relate mapping of phylogeny to biogeography only in very general terms. The Group A subclade may preferentially associate with the dimly lit waters near the NO_2^- maximum and, based on the results of this study, share comparable sensitivity to light. The biogeography of these two dominant lineages (OTU_2 and OTU_29 vs. OTU 5 and OTU_34) within this subclade of Group A appears to reflect the well-recognized chemical/physical separation of gyre and northern latitude waters. However, clarification of these relationships will require studies that more fully explore additional potential biotic and abiotic variables, and incorporate greater temporal and spatial resolution.

Photoinhibition of ammonia oxidation

Concurrent with many other reports, molecular evidence and results from the application of metabolic inhibitors strongly suggest that AOA are responsible for most, if not all, ammonia oxidation in these natural marine communities. Several studies have suggested that marine AOA in culture and those associated with natural communities are highly sensitive to sunlight (Mincer et al. 2007; Kalanetra et al. 2009; Church et al. 2010; Luo et al. 2014). However, only a few studies have quantified the photosensitivity, and the response by Group A *Thaumarchaeota* to light does not appear to be uniform. Light measurements in laboratory culture studies are conventionally reported in quantum flux (μE m^{-2} s^{-1}), while light measurements for field studies are reported in % surface PAR primarily because quantum flux is variable and more difficult to precisely quantify. Thus, direct comparisons between laboratory cultures and field studies can be difficult and there are different spectral qualities when comparing sunlight vs. artificial lamp sources. Qin et al. (2014) reported partial photoinhibition at light levels as low as 15 μE m^{-2} s^{-1} in three AOA laboratory cultures, and dark recovery of completely light-inhibited *N. maritimus* strain SCM1 cultures at 60 μE m^{-2} s^{-1}. A study of a natural marine community in the eastern tropical South Pacific dominated by AOA reported 66% photoinhibition at the 10% light level (Peng et al. 2016). In contrast, very different results were reported for another natural marine community in Monterey Bay Smith et al. (2014), in which samples incubated at 90% surface illumination were not fully inhibited and samples incubated at 50% surface light showed no

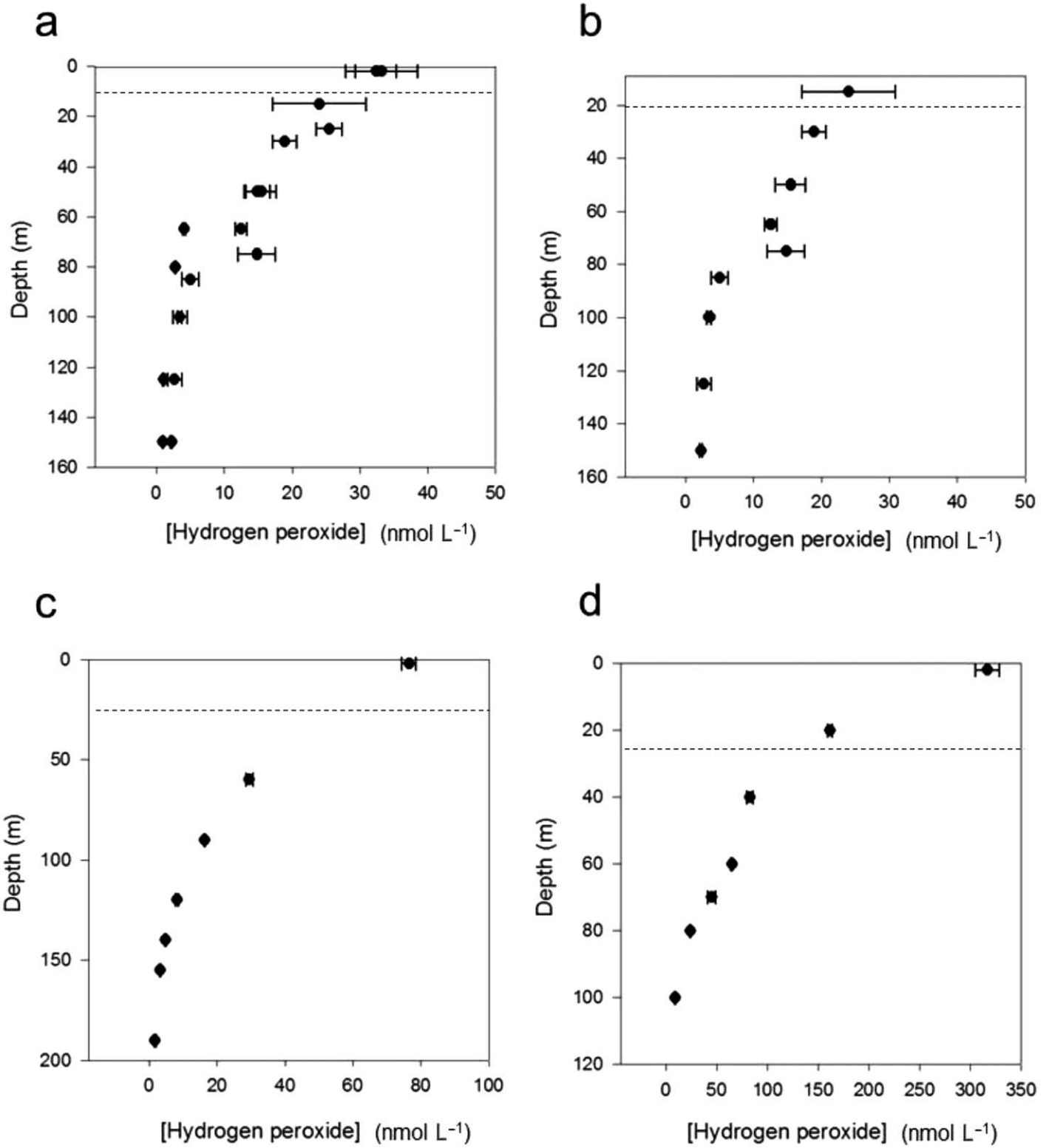

Fig. 7. Profiles of hydrogen peroxide at (**a**) Sta. 5, (**b**) Sta. 8, (**c**) Sta. 10, (**d**) Sta. 13. The dashed line is the mixed layer depth.

inhibition, implicating the Group A *Thaumarchaeota* as a "light tolerant ecotype" (Smith et al. 2014).

In the current study, measured ammonia oxidation rates in populations of AOA collected from or near the NO_2^- maximum across two North Pacific transects were shown to be highly sensitive to sunlight when incubated at sunlit depths. At all stations, ammonia oxidation rates in the light treatment increased with depth such that the highest rates of ammonia oxidation were at the incubation depths of the NO_2^- maximum and deeper. When comparing light and dark samples collected at a single discrete depth, all AOA communities had equal or nearly equal ammonia oxidation rates when incubated in clear and dark bottles and incubated at the NO_2^- maximum and deeper. This agreement among bottles incubated in the absence and presence of light is a good control on the experimental protocol because it suggests that clear and dark bottles experiencing the same conditions had similar rates.

Samples for the photoinhibition experiments were taken only at or near the NO_2^- maximum, which is usually the depth of the highest rates of ammonia oxidation and highest AOA cell counts in the water column. The results clearly show that the AOA populations at these depths are well-adapted to ammonia oxidation at low light levels. Without high-resolution sampling for AOA community diversity and photosensitivity, we are unable to comment on the light sensitivity of other AOA populations at different depths within the water column, including those at the surface. However, given that AOA cell counts and ammonia oxidation rates are generally very low in the upper water column (Mincer et al. 2007; Beman et al. 2012; Newell et al. 2013), it would be difficult to quantify photosensitivity there.

The incubation of clear bottles (light treatment) could potentially decrease the observed ammonia oxidation rate by stimulating phytoplankton N uptake of $^{15}NH_4^+$ or $^{15}NO_2^-$. Our data do suggest that ammonia uptake is not an important factor at most stations. Measured $^{15}NH_4^+$ uptake rates, which were incubated shipboard, could decrease the NH_4^+ pool by 2.8–89% during the course of incubation (Sta. 5: 8.0%; Sta. 8: 41.9%; Sta. 10: 89.1%; Sta. 13: 2.8%). These data indicate that competition for NH_4^+ between NH_4^+ uptake and ammonia oxidation should not affect the ammonia oxidation rate at Sta. 5, 8, and 13, but suggest that rates were depressed by high uptake observed at Sta. 10. The high ammonia uptake rates at Sta. 10 were unexpected based on low fluorescence readings at that depth. Although ammonia uptake might have inflated the apparent photoinhibition at this station by decreasing the available NH_4^+ in the light treatment and lowering rates in the clear bottles, the trend observed was in line with other stations. Nitrite uptake rates were 1–2 orders of magnitude lower than ammonia oxidation rates and were sufficient to deplete the NO_2^- pool by only 0.002–0.02% during the course of incubation (Sta. 5: 0.020%; Sta. 8: 0.002%; Sta. 10: 0.010%; Sta. 13: 0.014%).

The second N uptake experiment, the post-photoinhibition N uptake experiment conducted only at Sta. 13, also did not show evidence of NH_4^+ uptake being enhanced by light. At Sta. 13, NH_4^+ uptake in the light treatment was lower than NH_4^+ uptake in the dark treatment for incubations carried out at the surface and 12 m (Supporting Information Fig. S3), likely because of photoinhibition of a phytoplankton community not adapted to high light flux (Falkowski 1994). For incubations carried out at 60 m, 170 m, and 190 m, the NH_4^+ uptake rates for the light treatment in the post-photoinhibition N uptake experiment were similar to NH_4^+ uptake rates on experiments incubated shipboard (Supporting Information Table S3). Taken together, NH_4^+ and NO_2^- uptake rates measured at or around the depth of the photoinhibition experiment suggest that N uptake likely did not greatly affect ammonia oxidation rate measurements in light treatments.

We quantified the ammonia oxidation rate sensitivity to sunlight at four stations. There was nearly complete inhibition (95–100%) of ammonia oxidation at the surface and 6 m depth at Sta. 8 and 13, and around 80% photoinhibition at the surface and 6 m depth at Sta. 5 and 10 (Fig. 6). When all stations are considered, our regression analysis of % sPAR (surface PAR) and ammonia oxidation rate indicates that the AOA ammonia oxidation rate exhibits 25–41% inhibition at the 1% sPAR light level. Interestingly, Sta. 5, 10, and 13 had a statistically equal response to light, even though the AOA community compositions of Sta. 5 and 10 are quite different from those of Sta. 13 (Fig. 3; Supporting Information Fig. S1). While the striking differences in community structure likely play a role in the observed differences in photosensitivity, we cannot rule out the possibility that the different responses to light at least partially results from differences in physiological status among populations. For instance, it is possible that cells at Sta. 13 (oligotrophic gyre station) are under more nutritional stress than at other stations, and this could affect their response to light as an additional environmental stressor.

We found a greater degree of photoinhibition than other reports of photoinhibition for natural populations, but the difference between the PUV radiometer and CTD-mounted PAR sensor could account for at least some of the observed differences. The method of measuring light in this study contributes to dissimilarities in light response between this study and other studies that have reported the relationship between light and archaeal nitrification in the ocean (Smith et al. 2014; Peng et al. 2016). We used PUV-GUV paired radiometers that allow for a more direct measurement of light with depth and avoids assumptions including light attenuation through the air–water interface, which can vary significantly with time of day (Kirk 1994). In contrast, the 4π collector on the CTD-mounted PAR sensor integrates light from all directions including light from surface reflection, not just downwelling.

We also found that the NO_2^- maximum occurs at a much lower light level than the canonical 1% sPAR limit of the euphotic zone (0.07–0.24% sPAR). Given that the highest rates of nitrification are usually centered on the NO_2^- maximum, nitrification above the 1% sPAR level should be reconsidered in biogeochemical models as our data suggest that marine AOA communities still sustained 59–75% of ammonia oxidation activity at that light level. For instance, the National Center for Atmospheric Research Community Earth System Model (www.cesm.ucar.edu) assumes that nitrification is restricted at 2% sPAR, but our data shows that activity in *Thaumarchaea* are 42–64% of dark rates at that light.

Photoinhibition vs. H_2O_2 toxicity

Hydrogen peroxide addition of 50 nmol L^{-1} did not have a negative effect on ammonia oxidation rates in any of the samples we studied, suggesting that it is not an important factor within our study area (Supporting Information Table S2). To critically evaluate this conclusion, we also compare our data for H_2O_2 distribution with estimates of peroxide inhibition based on results from Tolar et al. (2016). In that study, H_2O_2 concentrations as little as 10 nmol L^{-1} were toxic to *Thaumarchaea* from the Southern Ocean (Tolar et al. 2016). In contrast, temperate ecotypes from Gulf of Alaska were much more resilient (Tolar et al. 2016), which is consistent with our results spanning two transects of North Pacific Ocean. There, the significant inhibitory effects were only reported at H_2O_2 concentrations greater than or equal to 100 nmol L^{-1} (Tolar et al. 2016), exceeding most of our reported concentrations except in surface waters at Sta. 10 and 13. So, we cannot exclude the possibility that H_2O_2 plays a role in ammonia oxidation inhibition in the surface waters with high H_2O_2 concentrations.

Vertical mixing of hydrogen peroxide, which has a long lifetime, could extend the effect of light inhibition below depths where direct photoinhibition becomes negligible. However, H_2O_2 concentrations below the mixed layer seldom exceeded 20 nmol L^{-1}, well below the concentration of 50 nmol L^{-1} that yielded no inhibition in the incubations. The physiological mechanism of photosensitivity in AOA has yet to be elucidated, but our evidence and growing evidence from other recent studies generally does not support that AOA photosensitivity results from the creation of H_2O_2 upon light incidence as has been suggested by other studies (Hollibaugh et al. 2011; Luo et al. 2014; Tolar et al. 2016). In addition, the H_2O_2 toxicity in *Thaumarchaea* cultures could be alleviated by the supplementation of α-keto acids or co-culturing with peroxidase-producing bacteria (Kim et al. 2016). Furthermore, single-cell genome analysis of epipelagic *Thaumarchaeota* populations showed the presence of putative catalase genes, coding for an efficient H_2O_2 scavenging enzyme (Luo et al. 2014). Interestingly, *N. maritimus* SCM1 is insensitive to typical environmental concentrations of H_2O_2 (Qin et al. 2017) in spite of the absence of catalase and peroxidase (Walker et al. 2010). However, in our re-inspection of the *N. maritimus* genome sequence, we identified two copies of superoxide dismutase (Nmar 0729 and Nmar 0394) and one copy of peroxiredoxin (Nmar 0560), which in concert with thioredoxin (available annotation of Nmar0230) and thioredoxin reductase (Nmar 0672) reduce peroxide to water (Walker et al. 2010). It is unknown how representative the insensitive response of *N. maritimus* to H_2O_2 is of other AOA strains.

The strong linear relationship between light and inhibition of ammonia oxidation hints that sunlight may impose damage to a key ammonia oxidation enzyme, as previously suggested for the AOB; photosensitivity of the AOB has been attributed to photo-oxidative damage of the copper-containing ammonia monooxygenase (reviewed in Ward 2013). However, this does not mean that H_2O_2 is unimportant. Tolar et al. (2016) make a convincing case that peroxide toxicity exerts significant selective pressure in southern polar regions, where as little as 10 nmol L^{-1} H_2O_2 was shown to inhibit ammonia oxidation. In addition, our results and those reported by Tolar et al. (2016), also reveal an increase in ammonia oxidation rates with peroxide. Five out of 15 of our incubations, and a comparable fraction of those in the study by Tolar et al. (2016), showed a positive effect of peroxide. We do not have a direct explanation for this effect, but it is possible that hydrogen peroxide has a negative effect on competitors of *Thaumarchaea* at these sites. This is supported by recent studies reported by Qin et al. (2017), demonstrating that some AOA are resistant to extremely high peroxide concentrations (> 1 μmol L^{-1}). Thus, our data indicate that direct irradiation exerts a more fundamental control on ammonia oxidation, at least in open ocean regimes, and that H_2O_2 would have a modest effect on ammonia oxidation within the mixed layer and a negligible effect below.

Variability in ecophysiology among closely related AOA

Variable responses to light and temperature among populations at the stations sampled likely reflect significant phenotypic plasticity among AOA affiliated with Group A. Our results suggest that communities of closely related AOA phylotypes can be affected differently by light and temperature. Ecotype variability may also help explain differences in Q_{10} measurements from previous studies (Horak et al. 2013; Baer et al. 2014). While the range of Q_{10} values for Sta. 5 (1.0), 8 (1.7), and 10 (1.0) are within the range of published Q_{10} values for other AOA assemblages in the field, Sta. 13 is an outlier with a very high Q_{10} (3.4). Stations 5 and 10 had very similar AOA population structure (Supporting Information Fig. S1) and also displayed the same temperature response. Similarly, oligotrophic gyre Sta. 13, with the most disparate Q_{10}, was dominated by OTUs primarily associated with stations in the oligotrophic gyre (OTU_5 and OTU_34). Hierarchical clustering of *amoA* gene phylotypes also provided

statistical support for differences in *amoA* gene communities observed in the gyre (Sta. 13, 14, 15, 16) and those located along the coastal and offshore transects (Sta. 1–8; Supporting Information Fig. S1). These data provide further support for differences in *amoA* phylotypes being associated with contrasting physical and chemical conditions that impact nitrification rates. This is the first evidence for varying temperature sensitivity among AOA genotypes in natural marine assemblages.

Correlations between AOA community structure and response to light and temperature were also observed. Rates of ammonia oxidation at Sta. 5 and 10, dominated by the same OTUs, showed comparable responses to light and were unaffected by differences in incubation temperature. Conversely, the distinctive divergence in community structure observed between Sta. 10 and 13 was only reflected in a dramatically different response to temperature (Q_{10}: 1.0, Sta. 10; 3.7, Sta. 13), not in sensitivity to light. Thus, the observed distinctive differences in light and temperature sensitivity among closely related natural populations of AOA suggests that ecotypic variation cannot be easily inferred solely from conventional sequence analysis.

Conclusions

Since the form and availability of nitrogen has major impacts on marine food webs, and since temperature and light attenuation are two variables under the influence of climate forcing, it is important to determine the sensitivity of oceanic nitrification to variation in those two major variables. Using a study design that resolved the differential influences of light, temperature, and peroxide on ammonia oxidation in open ocean communities dominated by *Thaumarchaeota*, photosensitivity was shown to the most important controlling variable. Furthermore, using precise PAR measurements, we could show that AOA ammonia oxidation rates are only partially inhibited by sunlight within the depths of the euphotic zone (defined by 1% surface PAR). The variability in sensitivity to light and temperature among closely related phylotypes also points to a fine scale niche differentiation that presumably sustains significant diversity in natural populations. Thus, although our data does extend understanding of thaumarchaeal phenotypic variability in response to environmental stressors, it also highlights the need to better define variation in adaptive capacity among the tremendous genetic diversity of populations sustaining this key biogeochemical process.

References

Amin, S., and others. 2013. Copper requirements of the ammonia-oxidizing archaeon *Nitrosopumilus maritimus* SCM1 and implications for nitrification in the marine environment. Limnol. Oceanogr. **58**: 2037–2045. doi:10.4319/lo.2013.58.6.2037

Baer, S., T. Connelly, R. Sipler, P. Yager, and D. Bronk. 2014. Effect of temperature on rates of ammonium uptake and nitrification in the western coastal Arctic during winter, spring, and summer. Global Biogeochem. Cycles **28**: 1455–1466. doi:10.1002/2013GB004765

Bayer, B., and others. 2016. Physiological and genomic characterization of two novel marine thaumarchaeal strains indicates niche differentiation. ISME J. **10**: 1051–1063. doi:10.1038/ismej.2015.200

Beman, J., B. Popp, and C. Francis. 2008. Molecular and biogeochemical evidence for ammonia oxidation by marine Crenarchaeota in the Gulf of California. ISME J. **2**: 429–441. doi:10.1038/ismej.2007.118

Beman, J., B. Popp, and S. Alford. 2012. Quantification of ammonia oxidation rates and ammonia-oxidizing archaea and bacteria at high resolution in the Gulf of California and eastern tropical Pacific Ocean. Limnol. Oceanogr. **57**: 711–726. doi:10.4319/lo.2012.57.3.0711

Bokulich, N. A., S. Subramanian, J. J. Faith, D. Gevers, J. I. Gordon, R. Knight, D. A. Mills, and J. G. Caporaso. 2013. Quality-filtering vastly improves diversity estimates from Illumina amplicon sequencing. Nat. Methods **10**: 57–59. doi:10.1038/nmeth.2276

Bristow, L., and others. 2016. Ammonium and nitrite oxidation at nanomolar oxygen concentrations in the oxygen minimum zone waters. Proc. Natl. Acad. Sci. USA **113**: 10601–10606. doi:10.1073/pnas.1600359113

Bronk, D., P. Glibert, and B. Ward. 1994. Nitrogen uptake, dissolved organic nitrogen release, and new production. Science **265**: 1843–1846. doi:10.1126/science.265.5180.1843

Church, M., B. Wai, D. Karl, and E. DeLong. 2010. Abundances of crenarchaeal *amoA* genes and transcripts in the Pacific Ocean. Environ. Microbiol. **12**: 679–688. doi:10.1111/j.1462-2920.2009.02108.x

Croot, P., P. Strue, I. Peeken, K. Lochte, and A. Baker. 2004. Influence of the ITCZ on H2O2 in near surface waters in the equatorial Atlantic Ocean. Geophys. Res. Lett. **31**: L23S04. doi:10.1029/2004GL020154

Daims, H., and others. 2015. Complete nitrification by *Nitrospira* bacteria. Nature **528**: 504–509. doi:10.1038/nature16461

Dugdale, R., and J. Goering. 1967. Uptake of new and regenerated forms of nitrogen in primary productivity. Limnol. Oceanogr. **12**: 196–206. doi:10.4319/lo.1967.12.2.0196

Edgar, R. 2010. Search and clustering orders of magnitude faster than BLAST. Bioinformatics **26**: 2460–2461. doi:10.1093/bioinformatics/btq461

Edgar, R. 2013. UPARSE: Highly accurate OTU sequences from microbial amplicon reads. Nat. Methods **10**: 996–998. doi:10.1038/nmeth.2604

Francis, C., K. Roberts, J. Beman, A. Santoro, and B. Oakley. 2005. Ubiquity and diversity of ammonia-oxidizing Archaea in water columns and sediments of the ocean. Proc. Natl. Acad. Sci. USA **102**: 14683–14688. doi:10.1073/pnas.0506625102

Grasshoff, K., K. Kremling, and M. Erhard. 1999. Methods of seawater analysis, 3rd ed. Wiley-VCH.

Heal, K., and others. 2017. Two distinct pools of B_{12} analogs reveal community interdependencies in the ocean. Proc. Natl. Acad. Sci. USA **114**: 364–369. doi:10.1073/pnas.1608462114

Heller, M., D. Gaiero, and P. Croot. 2013. Basin scale survey of marine humic fluorescence in the Atlantic: Relationship to iron solubility and H_2O_2. Global Biogeochem. Cycles **27**: 14. doi:10.1029/2012GB004427

Hollibaugh, J., S. Gifford, S. Sharma, N. Bano, and M. Moran. 2011. Metatranscriptomic analysis of ammonia-oxidizing organisms in an estuarine bacterioplankton assemblage. ISME J. **5**: 866–878. doi:10.1038/ismej.2010.172

Holmes, R., A. Aminot, R. Kerouel, B. Hooker, and B. Peterson. 1999. A simple and precise method for measuring ammonium in marine and freshwater ecosystems. Can. J. Fish. Aquat. Sci. **56**: 1801–1809. doi:10.1139/cjfas-56-10-1801

Horak, R. E. A., W. Qin, A. J. Schauer, E. V. Armbrust, A. E. Ingalls, J. W. Moffett, D. A. Stahl, and A. H. Devol. 2013. Ammonia oxidation kinetics and temperature sensitivity of a natural marine community dominated by Archaea. ISME J. **7**: 2023–2033. doi:10.1038/ismej.2013.75

Kalanetra, K., N. Bano, and J. Hollibaugh. 2009. Ammonia-oxidizing Archaea in the Arctic Ocean and Antarctic coastal waters. Environ. Microbiol. **11**: 2434–2445. doi:10.1111/j.1462-2920.2009.01974.x

Karner, M., E. DeLong, and D. Karl. 2001. Archaeal dominance in the mesopelagic zone of the Pacific Ocean. Nature **409**: 507–510. doi:10.1038/35054051

Kim, J.-G., and others. 2016. Hydrogen peroxide detoxification is a key mechanism for growth of ammonia-oxidizing archaea. Proc. Natl. Acad. Sci. USA **113**: 7888–7893. doi:10.1073/pnas.1605501113

Kirk, J. 1994. Light and photosynthesis in aquatic ecosystems, 2nd ed. Cambridge Univ. Press.

Long, S., S. Humphries, and P. Falkowski. 1994. Photoinhibition of photosynthesis in nature. Annu. Rev. Plant Biol. **45**: 633–662. doi:10.1146/annurev.pp.45.060194.003221

Lomas, M., and F. Lipschultz. 2006. Forming the primary nitrite maximum: Nitrifiers or phytoplankton? Limnol. Oceanogr. **51**: 2453–2467. doi:10.4319/lo.2006.51.5.2453

Ludwig, W., and others. 2004. ARB: A software environment for sequence data. Nucleic Acids Res. **32**: 1363–1371. doi:10.1093/nar/gkh293

Lunau, M., A. Lemke, K. Walther, W. Martens-Habbena, and M. Simon. 2005. An improved method for counting bacteria from sediments and turbid environments by epifluorescence microscopy. Environ. Microbiol. **7**: 961–968. doi:10.1111/j.1462-2920.2005.00767.x

Luo, H., B. B. Tolar, B. K. Swan, C. L. Zhang, R. Stepanauskas, M. Ann Moran, and J. T. Hollibaugh. 2014. Single-cell genomics shedding light on marine Thaumarchaeota diversification. ISME J. **8**: 732–736. doi:10.1038/ismej.2013.202

Martens-Habbena, W., P. Berube, H. Urakawa, J. de la Torre, and D. Stahl. 2009. Ammonia oxidation kinetics determine niche separation of nitrifying Archaea and Bacteria. Nature **461**: 976–979. doi:10.1038/nature08465

Martens-Habbena, W., and others. 2015. The production of nitric oxide by marine ammonia-oxidizing archaea and inhibition of archaeal ammonia oxidation by a nitric oxide scavenger. Environ. Microbiol. **17**: 2261–2274. doi:10.1111/1462-2920.12677

McIlvin, M., and M. Altabet. 2005. Chemical conversion of nitrate and nitrite to nitrous oxide for nitrogen and oxygen isotopic analysis in freshwater and seawater. Anal. Chem. (Wash.). **77**: 5589–5595. doi:10.1021/ac050528s

Mincer, T., M. Church, L. Trent Taylor, C. Preston, D. Karl, and E. DeLong. 2007. Quantitative distribution of presumptive archaeal and bacterial nitrifiers in Monterey Bay and the North Pacific Subtropical Gyre. Environ. Microbiol. **9**: 1162–1175. doi:10.1111/j.1462-2920.2007.01239.x

Newell, S., S. Fawcett, and B. Ward. 2013. Depth distribution of ammonia oxidation rates and ammonia-oxidizer community composition in the Sargasso Sea. Limnol. Oceanogr. **58**: 1491–1500. doi:10.4319/lo.2013.58.4.1491

Norton, J., J. Alzerreca, Y. Suwa, and M. Klotz. 2002. Diversity of ammonia monooxygenase operon in autotrophic ammonia-oxidizing bacteria. Arch. Microbiol. **177**: 139–149. doi:10.1007/s00203-001-0369-z

Nunora, T., and others. 2015. Hadal biosphere: Insight into the microbial ecosystem in the deepest ocean on Earth. Proc. Natl. Acad. Sci. USA **112**: E1230–E1236. doi:10.1073/pnas.1421816112

Peng, X., C. A. Fuchsman, A. Jayakumar, S. Oleynik, W. Martens-Habbena, A. H. Devol, and B. B. Ward. 2015. Ammonia and nitrite oxidation in the Eastern Tropical North Pacific. Global Biogeochem. Cycles **29**: 2034–2049. doi:10.1002/2015GB005278

Peng, X., C. Fuchsman, A. Jayakumar, M. Warner, A. Devol, and B. Ward. 2016. Revisiting nitrification in the Eastern Tropical South Pacific: A focus on controls. J. Geophys. Res. Oceans **121**: 1667–1684. doi:10.1002/2015JC011455

Pester, M., and others. 2012. amoA-based consensus phylogeny of ammonia-oxidizing archaea and deep sequencing of amoA genes from soils of four different geographic regions. Environ. Microbiol. **14**: 525–539. doi:10.1111/j.1462-2920.2011.02666.x

Qin, W., and others. 2014. Marine ammonia-oxidizing archaeal isolates display obligate mixotrophy and wide ecotypic variation. Proc. Natl. Acad. Sci. USA **111**: 12504–12509. doi:10.1073/pnas.1324115111

Qin, W., L. T. Carlson, E. V. Armbrust, A. H. Devol, J. W. Moffett, D. A. Stahl, and A. E. Ingalls. 2015*a*. Confounding effects of oxygen and temperature on the TEX86 signature of marine *Thaumarchaeota*. Proc. Natl. Acad. Sci. USA **112**: 10979–10984. doi:10.1073/pnas.1501568112

Qin, W., W. Martens-Habbena, J. Kobelt, and D. Stahl. 2015*b*. Candidatus nitrosopumilales. *In* W. B. Whitman [ed.], Bergey's manual of systematics of archaea and bacteria. John Wiley & Sons, Ltd.

Qin, W., W. Martens-Habbena, J. Kobelt, and D. Stahl. 2015*c*. Candidatus nitrosopumilus. *In* W. B. Whitman [ed.], Bergey's manual of systematics of archaea and bacteria. John Wiley & Sons, Ltd.

Qin, W., K. A. Meinhardt, J. W. Moffett, A. H. Devol, E. Virginia Armbrust, A. E. Ingalls, and D. A. Stahl. 2017. Influence of oxygen availability on the activities of ammonia-oxidizing Archaea. Environ. Microbiol. Rep. **9**: 250–256. doi:10.1111/1758-2229.12525

Rotthauwe, J. H., K. P. Witzel, and W. Liesack. 1997. The ammonia monooxygenase structural gene *amoA* as a functional marker: Molecular fine-scale analysis of natural ammonia-oxidizing populations. Appl. Environ. Microbiol. **63**: 4704–4712.

Santoro, A., K. Casciotti, and C. Francis. 2010. Activity, abundance, and diversity of nitrifying archaea and bacteria in the central California Current. Environ. Microbiol. **12**: 1989–2006. doi:10.1111/j.1462-2920.2010.02205.x

Santoro, A., and others. 2013. Measurements of nitrite production in and around the primary nitrite maximum in the central California Current. Biogeosciences **10**: 7395–7410. doi:10.5194/bg-10-7395-2013

Sauder, L., A. Ross, and J. Neufield. 2016. Nitric oxide scavengers differentially inhibit ammonia oxidation in ammonia-oxidizing archaea and bacteria. FEMS Microbiol. Lett. **363**. doi:10.1093/femsle/fnw052

Sintes, E., K. Bergauer, D. De Corte, T. Yokokawa, and G. Herndl. 2013. Archaeal *amoA* gene diversity points to distinct biogeography of ammonia-oxidizing *Crenarchaeota* in the ocean. Environ. Microbiol. **15**: 1647–1658. doi:10.1111/j.1462-2920.2012.02801.x

Smith, J., F. Chavez, and C. Francis. 2014. Ammonium uptake by phytoplankton regulates nitrification in the sunlit ocean. PLoS ONE **9**: e108173. doi:10.1371/journal.pone.0108173

Stieglmeier, M., R. Alves, and C. Schleper. 2014. The phylum Thaumarchaeota, p. 347–362. *In* M. Dworkin, S. Falkow, E. Rosenberg, K.-H. Schleifer, and E. Stackebrandt [eds.], The prokaryotes. Springer.

Tolar, B., L. Powers, W. Miller, N. Wallsgrove, B. Popp, and J. Hollibaugh. 2016. Ammonia oxidation in the ocean can be inhibited by nanomolar concentrations of hydrogen peroxide. Front. Mar. Sci. **3**: 237. doi:10.3389/fmars.2016.00237

UNESCO. 1994. Protocols for the Joint Global Ocean Flux Study (JGOFS) Core Measurements. IOC Manual and Guides 29.

Urakawa, H., W. Martens-Habbena, and D. Stahl. 2010. High abundance of ammonia-oxidizing Archaea in coastal waters determined using a modified DNA extraction method. Appl. Environ. Microbiol. **76**: 2129–2135. doi:10.1128/AEM.02692-09

van Kessel, M., D. R. Speth, M. Albertsen, P. H. Nielsen, H. J. Op den Camp, B. Kartal, M. S. Jetten, and S. Lücker. 2015. Complete nitrification by a single microorganism. Nature **528**: 555–559. doi:10.1038/nature16459

Walker, C., and others. 2010. *Nitrosopumilus maritimus* genome reveals unique mechanisms for nitrification and autotrophy in globally distributed marine crenarchaea. Proc. Natl. Acad. Sci. USA **107**: 8818–8823. doi:10.1073/pnas.0913533107

Ward, B. 1985. Light and substrate concentration relationships with marine ammonium assimilation and oxidation rates. Mar. Chem. **16**: 301–316. doi:10.1016/0304-4203(85)90052-0

Ward, B. 2011. Measurement and distribution of nitrification rates in the ocean. Methods Enzymol. **486**: 307–323. doi:10.1016/B978-0-12-381294-0.00013-4

Ward, B. 2013. Nitrification. In Reference module in Earth systems and environmental sciences. Elsevier. http://www.sciencedirect.com/science/article/pii/B9780124095489006977

Yool, A., A. Martin, C. Fernandez, and D. Clark. 2007. The significance of nitrification for oceanic new production. Nature **447**: 999–1002. doi:10.1038/nature05885

Yuan, J., and A. Shiller. 1999. Determination of subnanomolar levels of hydrogen peroxide in seawater by regent-injection chemiluminescence detection. Anal. Chem. (Wash.). **71**: 1975–1980. doi:10.1021/ac981357c

Acknowledgments

We would like to extend thanks to the following people for assistance with shipboard experiments and measurements: David French (also in situ array leader), Laura Carlson, Willow Coyote-Maestas, Chelsea McCurry. Kathy Krogsland and the UW Marine Chemistry lab provided excellent assistance with nutrient analysis. Thanks go to the captain and crew of the R/V *Kilo Moana* KM1314. Thanks go to Cheng Dang, Yue Zheng, and Wendi Ruef for technical assistance with figure preparation. This project was funded by National Science Foundation grants MCB-0604448 and Dimensions of Biodiversity Program OCE-1046017 to AHD, DAS, AEI, JWM, and EVA. Data for the cruise can be accessed through BCO-DMO accession numbers 539810 and 672310. The sequences reported in this paper have been deposited in the European Nucleotide Archive [accession no. PRJEB10943 (ERP012248) (project title "Variable Influence of light on the activity of *Thaumarchaea*")].

Conflict of Interest

None declared.

Submitted 14 March 2017
Revised 19 June 2017
Accepted 25 July 2017

Associate editor: Maren Voss